Adaptive Quasi-Dynamic Traffic Light Control

Julia L. Fleck, Christos G. Cassandras, *Fellow, IEEE*, and Yanfeng Geng, *Student Member, IEEE*

***Abstract*— We consider the traffic light control problem for a single intersection modeled as a stochastic hybrid system. We study a quasi-dynamic policy based on partial state information defined by detecting whether vehicle backlogs are above or below certain thresholds. The policy is parameterized by green and red cycle lengths as well as the road content thresholds. Using infinitesimal perturbation analysis, we derive online gradient estimators of a cost metric with respect to the controllable light cycles and threshold parameters and use these estimators to iteratively adjust all the controllable parameters through an online gradient-based algorithm so as to improve the overall system performance under various traffic conditions. The results obtained by applying this methodology to a simulated urban setting are also included.**

***Index Terms*— Optimization, perturbation analysis, stochastic hybrid systems (SHSs), traffic light control (TLC), traffic signal systems, transportation systems.**

I. Introduction

THE traffic light control (TLC) problem consists in adjusting green and red signal settings in order to control the traffic flow through an intersection and, more generally, through a set of intersections and traffic lights in an urban roadway network. The ultimate objective is to minimize congestion (hence delays experienced by drivers and resulting reductions in fuel usage and pollution) at a particular intersection, as well as an entire area consisting of multiple intersections. There are two types of control strategies for the TLC problem in the literature: fixed-time and traffic-responsive strategies. In the former, several timing plans covering different traffic intensity scenarios are periodically interchanged; for example, the urban traffic control system [48], TRANSYT [37], and MAXBAND [30] all make use of historical traffic flow data to determine light cycles offline and cannot adapt in real time to evolving traffic conditions. Traffic-responsive strategies address this limitation by making use of current traffic information to determine optimal signal settings online. They employ algorithms that adjust a signal's phase length and phase sequences so as to minimize delays and reduce the number of stops, requiring transit surveillance, typically implemented using pavement loop detectors, in order to adjust signal timing in real time. SCATS [32] and SCOOT [29] are two well-known examples of traffic control systems that implement traffic-responsive strategies.

Recent technological developments, which exploit the ability to collect traffic data in real time, have made it possible for new methods to be applied to the TLC problem, resulting in systems such as OPAC [20], PRODYN [26], RHODES [39], and ACS Lite [40]. Leveraging the fact that TLC is fundamentally a form of scheduling for systems operating through simple switching control actions, numerous solution algorithms have been proposed and we briefly review some of them next. Fuzzy logic was first used in [34] for a single intersection without turning traffic, and in [8], a fuzzy logic controller was presented capable of coping with traffic congestion over multiple intersections. Expert systems were used in [15], [16], and [46] to design TLC systems with features such as distributed control and an ability to deal with congested traffic. Evolutionary algorithms such as genetic algorithms [31], swarm optimization algorithms [10], [11], and ant algorithms [47] have also been proposed. Several approaches using artificial neural networks have been reported in [12], [27], and [41]. Reinforcement learning has also been used for TLC within a Markov decision process (MDP) framework, as reported in [1], [3], [39], and [46]. A discrete-time stationary MDP framework was also used in [52] to develop an adaptive control model of a network of signalized intersections. A game theoretic approach was applied to a finite controlled Markov chain model in [2]. In [35], a decision tree model was used with a rolling horizon dynamic programming approach, while a multiobjective mixed integer linear programming formulation was proposed in [14]. Optimal TLC was also stated as a special case of an extended linear complementarity problem in [38] and formulated as a hybrid system optimization problem in [53]. Robust optimization methods that take into account uncertain traffic flows have also been proposed. For example, in [42], a semidefinite programming routine for model predictive control is used; in [44], a robust optimal signal control problem is formulated as a linear program; in [51], signal timings were determined so as to minimize the mean delay per vehicle under daily traffic flow variations.

The aforementioned methods for real-time adaptive traffic control must address two main issues: 1) the development of a mathematical model for a stochastic and highly nonlinear traffic system and 2) the design of appropriate control laws. Although most existing adaptive signal control strategies implicitly recognize that variations in traffic conditions are

Manuscript received December 9, 2014; revised May 8, 2015; accepted July 27, 2015. Date of publication August 28, 2015; date of current version April 18, 2016. Manuscript received in final form August 4, 2015. This work was supported in part by the National Science Foundation under Grant CNS-1239021 and Grant IIP-1430145, in part by the Air Force Office of Scientific Research under Grant FA9550-12-1-0113, in part by the Office of Naval Research under Grant N00014-09-1-1051, and in part by the Cyprus Research Promotion Foundation through the New Infrastructure Project/Strategic/0308/26. Recommended by Associate Editor F. Basile.

J. L. Fleck and C. G. Cassandras are with the Division of Systems Engineering, Center for Information and Systems Engineering, Boston University, Brookline, MA 02446 USA (e-mail: jfleck@bu.edu; cgc@bu.edu).

Y. Geng is with Amazon, Boston, MA 02138 USA (e-mail: gengyf@bu.edu).

Color versions of one or more of the figures in this paper are available online at http://ieeexplore.ieee.org.

Digital Object Identifier 10.1109/TCST.2015.2468181

caused by random processes, they frequently resort to using deterministic models, which significantly simplify the description of vehicle flow. In addition, heuristic control strategies are also commonly employed for TLC without an embedded traffic flow model, as in the case of artificial intelligence techniques, which rely on historical data. Such applications are, as a result, better suited for traffic systems in steady state, which is in fact seldom attained. Stochastic control approaches address this limitation by explicitly accounting for the random variations in traffic flow, typically within an MDP framework, which requires specific probabilistic models. Furthermore, many of these approaches, such as those based on dynamic programming, are computationally inefficient, thus not immediately amenable to online implementations. In contrast to the above, perturbation analysis techniques [5] are entirely data driven and allow for stochastic control with no explicit traffic model required. They have proven to be adaptive and easily implementable online.

Perturbation analysis was used in [18] and [25] based on modeling a traffic light intersection as a stochastic discrete event system (DES). An infinitesimal perturbation analysis (IPA) approach, using a stochastic flow model (SFM) to represent the queue content dynamics of roads at an intersection, was presented in [33]. IPA was also applied with respect to controllable green and red phase times for a single isolated intersection in [22] and for multiple intersections in [21] and [24]. Modeling traffic flow through an intersection controlled by switching traffic lights as an SFM conveniently captures the system's inherent hybrid nature: while traffic light switches exhibit event-driven dynamics, the flow of vehicles through an intersection is best represented using time-driven dynamics. Moreover, traffic flow rates need not be restricted to take on deterministic values, but may be treated as stochastic processes [6], which are suited to represent the continuous random variations in traffic conditions. Using the general IPA theory for stochastic hybrid systems (SHSs) in [7] and [45], online gradients of performance measures may be estimated with respect to several controllable parameters with only minor technical conditions imposed on the random processes that define input and output flows at an intersection. Note that the purpose of IPA is not to estimate performance measures themselves, but only their gradients, which may be subsequently incorporated into standard gradient-based algorithms in order to effectively control parameters of interest. In particular, we stress that the IPA estimates obtained do not depend on any modeling assumptions for random traffic processes and involve only directly observable data.

There are several advantages associated with the use of IPA for the TLC problem:

1) IPA estimates have been shown to be unbiased under very mild conditions [50].
2) IPA estimators are robust with respect to the stochastic processes used in our model [4]. This is particularly relevant in the context of TLC, since the vehicle arrival and departure processes are intrinsically random.
3) IPA is event driven and hence scalable in the number of events in the system (generally manageable), and does not explode with the space dimensionality.

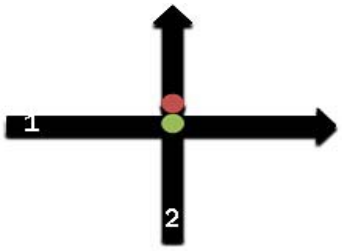

Fig. 1. Single traffic light intersection with two cross roads.

4) IPA possesses a decomposability property [4], i.e., IPA state derivatives become memoryless after certain events take place.
5) The IPA methodology can be easily implemented online, allowing us to take advantage of directly observed data.

In contrast to [9], [19], and [28] where the adjustment of light phases did not make use of real-time state information, a *quasi-dynamic* control setting was proposed in [23] in which partial state information is used to adjust the green and red light times conditioned upon a given queue content threshold being reached. A complementary approach, in which a quasi-dynamic policy is used to control the threshold parameters while assuming fixed phase times, is presented in [17]. Building upon these results, here we derive IPA performance measure estimators necessary to *simultaneously* optimize phase times and queue content threshold values within a quasi-dynamic control setting.

From a practical perspective, the goal of this paper is to present the basic IPA techniques applied to efficient adaptive traffic signal control using real-time information. Therefore, we introduce the relevant concepts related to an IPA-based TLC system ignoring several traffic engineering details which we believe can be readily incorporated into the proposed controller, as further discussed in Section III-C.

The remainder of this paper is organized as follows. In Section II, we formulate the TLC problem for a single intersection and present the modeling framework used throughout our analysis for controlling green and red phase lengths and vehicle queue thresholds. Section III details the derivation of an IPA estimator for the cost function gradient with respect to a controllable parameter vector defined by the green and red phase lengths and threshold parameters. The IPA estimator is then incorporated into a gradient-based optimization algorithm, and a number of implementation issues are discussed. We include the simulation results in Section IV, showing how the proposed quasi-dynamic control offers considerable improvement over prior results. Finally, we conclude and discuss future work in Section V.

II. Problem Formulation

We consider a single intersection, as shown in Fig. 1. For simplicity, left-turn and right-turn traffic flows are not considered and yellow light times are implicitly accounted for within a red phase. This system involves a number of stochastic processes that are all defined on a common probability space (Ω, F, P). Each road is modeled as a queue with a random *arrival flow process* $\{\alpha_n(t)\}$, $n = 1, 2$, where $\alpha_n(t)$ is the instantaneous vehicle arrival rate at time t. When the traffic

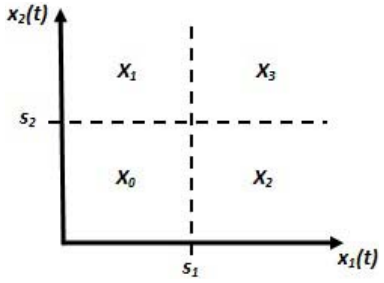

Fig. 2. State-space representation.

light corresponding to road n is GREEN, the *departure flow process* is denoted by $\{\beta_n(t)\}$, $n = 1, 2$. We define a state vector $x(t) = [x_1(t), x_2(t)]$, where $x_n(t) \in \mathbb{R}^+$ is the flow content of queue i, and assign to each queue n a guaranteed minimum GREEN light length $\theta_{n,\min}$ and a maximum length $\theta_{n,\max}$. For each queue n, we also define a clock state variable $z_n(t)$, $n = 1, 2$, which measures the time since the last switch from RED to GREEN of the traffic light for queue n, so that $z_n(t) \in [0, \theta_{n,\max}]$. Setting $z(t) = [z_1(t), z_2(t)]$, the complete system state vector is $[x(t), z(t)]$.

A *dynamic* controller is one that makes full use of the state information $z(t)$ and $x(t)$. Obviously, $z(t)$ is the controller's known internal state, but the queue content state is generally not instantaneously observable. We assume, however, that it is *partially* observable. Specifically, we can only observe whether $x_n(t)$ is below or above some threshold s_n, $i = 1, 2$. This is consistent with actual traffic systems where sensors, e.g., inductive loop detectors, are installed at each road near the intersection. Moreover, there is a growing trend toward exploiting connected vehicle technology to infer state variables $x_n(t)$ from data (e.g., location and speed) wirelessly exchanged through vehicle-to-vehicle or vehicle-to-infrastructure communication [13]. In this context, we shall define a *quasi-dynamic* controller where the controllable parameter vector of interest is given by

$$\upsilon = [\theta_{1,\min}, \theta_{1,\max}, \theta_{2,\min}, \theta_{2,\max}, s_1, s_2] \tag{1}$$

where $\theta_{n,\min} \geq 0$ and $\theta_{n,\max} > \theta_{n,\min}$ were defined above and $s_n \in \Re^+$ is a queue content threshold value for road $n = 1, 2$ whose precise function is explained next. The notation $x(\upsilon, t) = [x_1(\upsilon, t), x_2(\upsilon, t)]$ is used to stress the dependence of the state on the six controllable parameters. However, for notational simplicity, we will henceforth write $x(t)$ when no confusion arises; the same applies to $z(t)$.

Let us now partition the queue content state space into the following four regions (as shown in Fig. 2):

$$\begin{aligned} X_0 &= \{(x_1, x_2) : x_1(t) < s_1,\ x_2(t) < s_2\} \\ X_1 &= \{(x_1, x_2) : x_1(t) < s_1,\ x_2(t) \geq s_2\} \\ X_2 &= \{(x_1, x_2) : x_1(t) \geq s_1,\ x_2(t) < s_2\} \\ X_3 &= \{(x_1, x_2) : x_1(t) \geq s_1,\ x_2(t) \geq s_2\}. \end{aligned}$$

At any time t, the feasible control set for the traffic light controller is $U = \{1, 2\}$ and the control is defined as

$$u(x(t), z(t)) \equiv \begin{cases} 1, & \text{i.e., set road 1 GREEN, road 2 RED} \\ 2, & \text{i.e., set road 2 GREEN, road 1 RED.} \end{cases} \tag{2}$$

We define a *quasi-dynamic* controller of the form $u(X(t), z(t))$, with $X(t) \in \{X_0, X_1, X_2, X_3\}$, as follows:

for $X(t) \in \{X_0, X_3\}$

$$u(z(t)) = \begin{cases} 1, & \text{if } z_1(t) \in (0, \theta_{1,\max}) \text{ and } z_2(t) = 0 \\ 2, & \text{otherwise} \end{cases} \tag{3}$$

for $X(t) = X_1$

$$u(z(t)) = \begin{cases} 1, & \text{if } z_1(t) \in (0, \theta_{1,\min}) \text{ and } z_2(t) = 0 \\ 2, & \text{otherwise} \end{cases} \tag{4}$$

for $X(t) = X_2$

$$u(z(t)) = \begin{cases} 2, & \text{if } z_2(t) \in (0, \theta_{2,\min}) \text{ and } z_1(t) = 0 \\ 1, & \text{otherwise.} \end{cases} \tag{5}$$

This is a simple form of hysteresis control to ensure that the nth traffic flow always receives a minimum GREEN light time $\theta_{n,\min}$. Clearly, the GREEN phase may be dynamically interrupted anytime after $\theta_{n,\min}$ based on the partial state feedback provided through $X(t)$. For instance, if a transition into X_1 occurs while $u(X(t), z(t)) = 1$ and $z_1(t) > \theta_{1,\min}$, then the light switches from GREEN to RED for road 1 in order to accommodate an increasing backlog $x_2(t) \geq s_2$ at road 2. For notational simplicity, we will write $u(t)$ when no confusion arises, as we do with $x(t)$ and $z(t)$.

We can now write the dynamics of the state variables $x_n(t)$ and $z_n(t)$, starting with the observation that the departure flow process $\beta_n(t)$ on road n is given by

$$\beta_n(t) = \begin{cases} h_n(X(t), z(t), t), & \text{if } x_n(t) > 0 \text{ and } u(t) = n \\ \alpha_n(t), & \text{if } x_n(t) = 0 \text{ and } u(t) = n \\ 0, & \text{otherwise} \end{cases} \tag{6}$$

where $h_n(X(t), z(t), t)$ [subsequently also written as $h_n(t)$] is the instantaneous vehicle departure rate at time t, which generally depends on the specifics of the intersection and vehicle behavior. Then, adopting the notation $\bar{n}$ to denote the index of the road perpendicular to road $n = 1, 2$, we have

$$\dot{x}_n(t) = \begin{cases} \alpha_n(t), & \text{if } z_n(t) = 0 \\ 0, & \text{if } x_n(t) = 0 \text{ and } \alpha_n(t) \leq h_n(t) \\ \alpha_n(t) - \beta_n(t), & \text{otherwise} \end{cases} \tag{7}$$

$$\dot{z}_n(t) = \begin{cases} 1, & \text{if } z_{\bar{n}}(t) = 0 \\ 0, & \text{otherwise} \end{cases} \tag{8}$$

$$\begin{aligned} &z_n(t^+) = 0 \\ &\text{if } z_n(t) = \theta_{n,\max} \\ &\text{or } z_n(t) = \theta_{n,\min}, \quad x_n(t) < s_n, \quad x_{\bar{n}}(t) \geq s_{\bar{n}} \\ &\text{or } z_n(t) > \theta_{n,\min}, \quad x_n(t^-) > s_n, \quad x_n(t^+) = s_n, \quad x_{\bar{n}}(t) \geq s_{\bar{n}} \\ &\text{or } z_n(t) > \theta_{n,\min}, \quad x_n(t) < s_n, x_{\bar{n}}(t^-) < s_{\bar{n}}, \quad x_{\bar{n}}(t^+) = s_{\bar{n}}. \end{aligned}$$

Observe that $z_n(t)$ is discontinuous in t when the light switches from GREEN to RED on road n, since at this point, the GREEN cycle clock is reset to zero.

Thus, the traffic light intersection in Fig. 1 can be viewed as a hybrid system in which the time-driven dynamics are

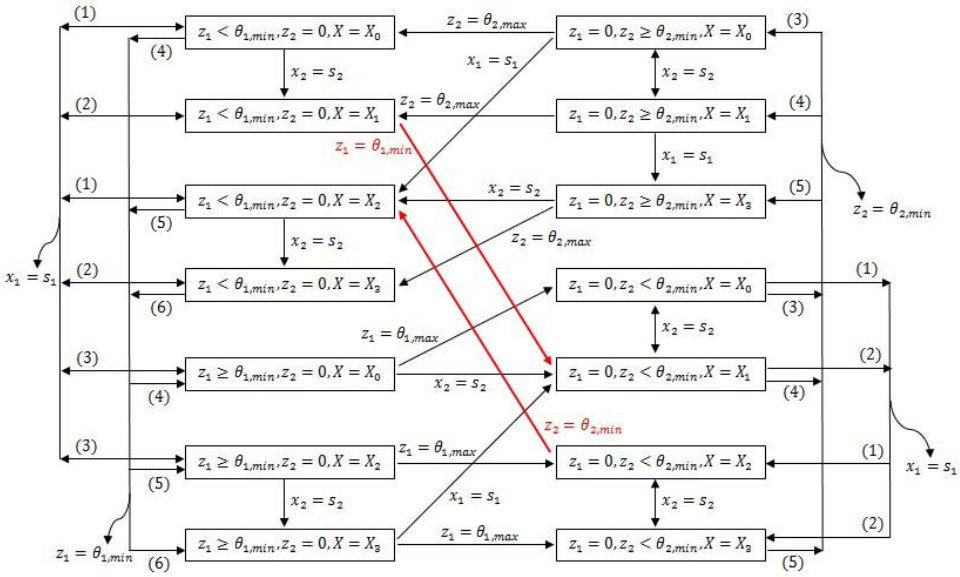

Fig. 3. SHA under quasi-dynamic control.

given by (7) and (8) and the event-driven dynamics are associated with light switches and with events that cause the value of $x_n(t)$ to change from strictly positive to zero or vice versa, or to cross the threshold s_n. It is then possible to derive a stochastic hybrid automaton (SHA) model as in [23] containing 14 modes, which are defined by combinations of $x_n(t)$ and $z_n(t)$ values. A simplified model, in which the state variable dynamics have been omitted and the states $x_n(t) = 0$ and $x_n(t) > 0$ have been combined into a single one, is shown in Fig. 3. The event set for this SHA is $\Phi = \Phi_1 \cup \Phi_2$, where $\Phi_n = \{\zeta_n^b, \zeta_n^a, \lambda_n, \mu_n, \chi_n, \gamma_n^1, \gamma_n^2\}$ and the subscript n refers to the road where the event occurred. The seven events in Φ_n are defined as follows.

1) ζ_n^b is the guard condition [$x_n = s_n$ from below].
2) ζ_n^a is the guard condition [$x_n = s_n$ from above].
3) λ_n is the guard condition [$z_n = \theta_{n,\min}$].
4) μ_n is the guard condition [$z_n = \theta_{n,\max}$].
5) χ_n is the guard condition [$x_n = 0$ from above].
6) γ_n^1 is a switch in the sign of $\alpha_n(t) - h_n(t)$ from nonpositive to strictly positive.
7) γ_n^2 is a switch in the sign of $\alpha_n(t)$ from 0 to strictly positive.

Note that the first four events $\{\zeta_n^b, \zeta_n^a, \lambda_n, \mu_n\}$ are those that induce light switches. In fact, if we label light switching events from RED to GREEN and GREEN to RED as $R2G_n$ and $G2R_n$, respectively, we can specify the following rules for our hysteresis-based quasi-dynamic controller corresponding to (3)–(5).

R1: The occurrence of event ζ_n^b, while $z_{\bar{n}} > \theta_{\bar{n},\min}$ and $x_{\bar{n}} < s_{\bar{n}}$, results in event $R2G_n$.

R2: The occurrence of event ζ_n^a, while $z_n > \theta_{n,\min}$ and $x_{\bar{n}} \geq s_{\bar{n}}$, results in event $G2R_n$.

R3: The occurrence of event λ_n, while $x_n < s_n$ and $x_{\bar{n}} \geq s_{\bar{n}}$, results in event $G2R_n$.

R4: The occurrence of event μ_n always results in event $G2R_n$.

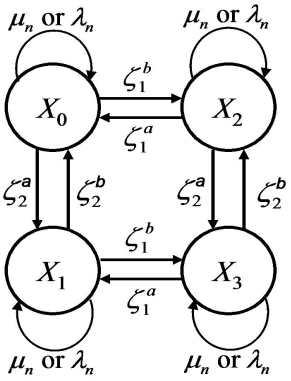

Fig. 4. SHA for aggregate states $X(t)$ under quasi-dynamic control.

A partial state transition diagram defined in terms of the aggregate queue content states $X(t)$ is shown in Fig. 4. A complete state transition diagram for this SHA is too complicated to draw and is not necessary for IPA. In fact, IPA focuses on analyzing a typical sample path of the SHA and, specifically, observable events in it. An example of such a sample path is shown in Fig. 5. Observe that any such sample path consists of alternating nonempty periods (NEPs) and empty periods (EPs), which correspond to time intervals when $x_n(t) > 0$ (i.e., queue n is nonempty) and $x_n(t) = 0$ (i.e., queue n is empty), respectively. Let us then label the events corresponding to the end and to the start of an NEP as E_n and S_n, respectively, and note that E_n is induced by event χ_n, while S_n may be induced by γ_n^1 or γ_n^2 or by a $G2R_n$ event.

Let us denote the mth NEP in a sample path of queue n by $[\xi_{n,m}, \eta_{n,m})$, where $\xi_{n,m}$, $m = 1, 2, \ldots$, is the occurrence time of the mth S_n event and $\eta_{n,m}$ is the occurrence time of the mth E_n event, as shown in Fig. 5. In addition, let the time of a light switching event (either $R2G_n$ or $G2R_n$) within the mth NEP be denoted by $t_{n,m}^j$, $j = 1, \ldots, J_m$.

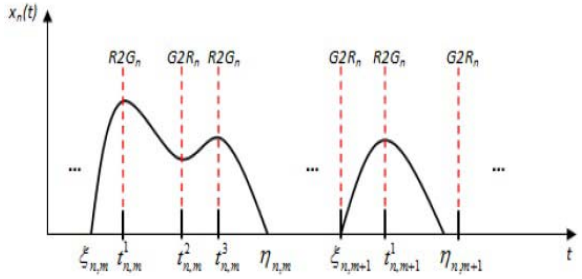

Fig. 5. Typical sample path of a traffic light queue.

Recall that the purpose of our analysis is to apply IPA to sample path data in order to obtain *online* unbiased gradient estimates of a system performance measure with respect to the controllable parameter vector υ and subsequently incorporate such estimates into an *online* gradient-based optimization scheme. In this context, let us choose our performance metric to be the weighted mean of the queue lengths over a fixed time interval $[0, T]$ and define the following sample function:

$$L(\upsilon; x(0), z(0), T) = \frac{1}{T}\sum_{n=1}^{2}\int_0^T w_n x_n(\upsilon, t)dt \tag{9}$$

where w_n is a weight associated with road n (i.e., its relative importance) and $x(0)$ and $z(0)$ are the given initial conditions. Since $x_n(t) = 0$ during EPs of road n, (9) can be rewritten as

$$L(\upsilon; x(0), z(0), T) = \frac{1}{T}\sum_{n=1}^{2}\sum_{m=1}^{M_n}\int_{\xi_{n,m}}^{\eta_{n,m}} w_n x_n(\upsilon, t)dt \tag{10}$$

where M_n is the total number of NEPs during the sample path of road n. Finally, let us define the overall performance metric as the expected weighted mean queue length

$$J(\upsilon; x(0), z(0), T) = E[L(\upsilon; x(0), z(0), T)]. \tag{11}$$

We note that it is not possible to derive a closed-form expression of $J(\upsilon; x(0), z(0), T)$ without full knowledge of the processes $\{\alpha_n(t)\}$ and $\{\beta_n(t)\}$. Even if $\{\alpha_n(t)\}$ and $\{\beta_n(t)\}$ were fully specified, evaluating the expectation $E[L(\upsilon; x(0), z(0), T)]$ is infeasible except for very simple cases. Therefore, a closed-form expression for $\nabla J(\upsilon)$ is also infeasible and the usual approach is to approximate derivatives such as $\partial J/\partial \upsilon_i$ by estimating $J(\upsilon_i; x(0), z(0), T)$ and $J(\upsilon_i + \delta; x(0), z(0), T)$ normally through repeated simulation, and use $[\hat{J}(\upsilon_i; x(0), z(0), T) - \hat{J}(\upsilon_i + \delta; x(0), z(0), T)]/\delta$ as such an approximation [where $\hat{J}(\cdot)$ is an estimate of $J(\cdot)$]. Clearly, this is extremely time consuming and potentially inaccurate since it depends on the choice of δ. The value of IPA lies in obtaining unbiased estimates of $\partial J/\partial \upsilon_i$ based only on data directly observable along a *single* sample path of the underlying SHS [5]. Moreover, multiple such estimates of $\partial J/\partial \upsilon_i$ for $i = 1, \ldots, n$ (the parameter vector dimensionality) can be concurrently obtained along this single sample path. Thus, by assuming only that $\alpha_n(t)$ and $h_n(t)$ are piecewise continuous w.p. 1, we can apply the IPA methodology developed for general SHS in [7] to the specific system at hand and obtain an estimate of $\nabla J(\upsilon)$ by evaluating the sample gradient $\nabla L(\upsilon)$. We emphasize that *no explicit knowledge of* $\alpha_n(t)$ and $h_n(t)$ *is necessary to estimate* $\nabla J(\upsilon)$. As will become clear in the sequel, it is only observable event counters and timers that are involved in obtaining an unbiased estimate of this gradient, which can then be used to improve current operating conditions or (under certain technical conditions) to compute an optimal υ^* through an iterative optimization algorithm of the form

$$\upsilon_{i,l+1} = \upsilon_{i,l} - \rho_l H_{i,l}(\upsilon_l, x(0), T, \omega_l) \tag{12}$$

where ρ_l is the step size at the lth iteration, $l = 0, 1, \ldots$, and ω_l denotes a sample path from which data are extracted and used to compute $H_{i,l}(\upsilon_l, x(0), T, \omega_l)$ defined to be an estimate of $dJ/d\upsilon_i$. We will further assume that the derivatives $dL/d\upsilon_i$ exist w.p. 1 for all $\upsilon_i \in \Re^+$. It is also easy to check that $L(\upsilon)$ is Lipschitz continuous for $\upsilon_i \in \Re^+$. Under these conditions, it has been shown in [7] that $dL/d\upsilon_i$ is indeed an unbiased estimator of $dJ/d\upsilon_i$, $i = 1, 2$.

III. Infinitesimal Perturbation Analysis

For the sake of completeness, we provide here a brief overview of the IPA framework developed for SHS in [7]. Consider a sample path of such a system over $[0, T]$ and denote the time of occurrence of the kth event (of any type) by $\tau_k(\theta)$, where, for simplicity, we take θ to be a scalar controllable parameter of interest. Let us also denote the state and event time derivatives with respect to parameter θ by

$$x'(\theta, t) \equiv \frac{\partial x(\theta, t)}{\partial \theta}, \quad \tau_k'(\theta) \equiv \frac{\partial \tau_k(\theta)}{\partial \theta}$$

respectively, for $k = 1, \ldots, N$. The dynamics of $x(\theta, t)$ are fixed over any interevent interval $[\tau_k(\theta), \tau_{k+1}(\theta))$, and we write $\dot{x}(\theta, t) = f_k(\theta, x, t)$ to represent the state dynamics over this interval. Although θ is included as an argument in the expressions above to stress the dependence on the controllable parameter, we will subsequently drop this for ease of notation as long as no confusion arises. It is shown in [7] that the state derivative satisfies

$$\frac{d}{dt}x'(t) = \frac{\partial f_k(t)}{\partial x}x'(t) + \frac{\partial f_k(t)}{\partial \theta} \tag{13}$$

with the following boundary condition:

$$x'(\tau_k^+) = x'(\tau_k^-) + \left[f_{k-1}(\tau_k^-) - f_k(\tau_k^+)\right] \cdot \tau_k'. \tag{14}$$

In order to evaluate (14), we must first determine τ_k', whose expression depends on the type of event that takes place at τ_k. As detailed in [7], the following three types of events are defined for a general SHS:

1) *Exogenous Events:* These events cause a discrete state transition that is independent of parameter θ and, as a result, satisfy $\tau_k' = 0$.
2) *Endogenous Events:* In this case, there exists a continuously differentiable function $g_k : \mathbb{R}^n \times \Theta \to \mathbb{R}$ such that $\tau_k = \min\{t > \tau_{k-1} : g_k(x(\theta, t), \theta) = 0\}$, where the function g_k usually corresponds to a guard condition in

a hybrid automaton. Taking derivatives with respect to θ, it is straightforward to obtain

$$\tau_k' = -\left[\frac{\partial g_k}{\partial x}\cdot f_{k-1}\left(\tau_k^-\right)\right]^{-1}\cdot\left(\frac{\partial g_k}{\partial \theta}+\frac{\partial g_k}{\partial x}\cdot x'\left(\tau_k^-\right)\right) \tag{15}$$

where $(\partial g_k/\partial x)\cdot f_{k-1}(\tau_k^-)\neq 0$.

3) *Induced Events:* Such an event occurs at time τ_k if it is triggered by the occurrence of another event at time $\tau_m \leq \tau_k$ so that the expression of τ_k' depends on that of τ_m' (the details can be found in [7]).

Clearly, IPA captures how changes in the controllable parameter affect the event times and the state of the system. Since interesting performance metrics are usually expressed in terms of τ_k and $x(\theta,t)$, IPA can ultimately be used to infer the effect that a perturbation in θ will have on such metrics.

Returning to our TLC problem, let us define the derivatives of the states $x_n(\upsilon,t)$ and $z_n(\upsilon,t)$ and event times $\tau_k(\upsilon)$ with respect to υ_i, $i=1,\ldots,6$, as follows:

$$x_{n,i}'(t)\equiv\frac{\partial x_n(\upsilon,t)}{\partial \upsilon_i},\quad z_{n,i}'(t)\equiv\frac{\partial z_n(\upsilon,t)}{\partial \upsilon_i},\quad \tau_{k,i}'\equiv\frac{\partial \tau_k(\upsilon)}{\partial \upsilon_i}. \tag{16}$$

Furthermore, since our complete system state vector is $[x(t),z(t)]$, let us denote the state dynamics over any interevent interval $[\tau_k(\theta),\tau_{k+1}(\theta))$ as follows:

$$\dot{x}_n(t)=f_{n,k}^x(t),\quad \dot{z}_n(t)=f_{n,k}^z(t),\quad n=1,2. \tag{17}$$

We end this overview by noting that, based on (7), we have

$$\frac{\partial f_{n,k}^x(t)}{\partial x_n}=\frac{\partial f_{n,k}^x(t)}{\partial \upsilon_i}=0$$

for $n=1,2$, $i=1,\ldots,6$, so that in (13), we have $(d/dt)x'(t)=0$ for $t\in[\tau_k,\tau_{k+1})$. Similarly, for the clock state variable $z_n(\upsilon,t)$, we have

$$\frac{\partial f_{n,k}^z(t)}{\partial z_n}=\frac{\partial f_{n,k}^z(t)}{\partial \upsilon_i}=0$$

for $n=1,2$, $i=1,\ldots,6$, and $(d/dt)z'(t)=0$ for $t\in[\tau_k,\tau_{k+1})$. This means that the value of the state derivative of any road remains unaltered while the system is in a given discrete mode

$$\begin{aligned} x_n'(t)&=x_n'\left(\tau_k^+\right),\quad t\in[\tau_k,\tau_{k+1})\\ z_n'(t)&=z_n'\left(\tau_k^+\right),\quad t\in[\tau_k,\tau_{k+1}). \end{aligned} \tag{18}$$

In what follows, the IPA expressions for state and event time derivatives will be derived for the events identified in our SHA model using (14), (15), and (18).

A. State and Event Time Derivatives

We proceed by considering each of the event types ($G2R_n$, $R2G_n$, E_n, and S_n) identified in the previous section as causing state transitions in either $x_n(t)$ or $z_n(t)$, $n=1,2$, and deriving the corresponding event time and state derivatives. We start by presenting a general result that applies to all the light switching events $G2R_n$ and $R2G_n$. Let us denote the time of occurrence of the jth light switching event by σ_j and define its derivative with respect to the control parameters as $\sigma_{j,i}'\equiv(\partial\sigma_j/\partial\upsilon_i)$, $i=1,\ldots,6$.

Proposition 1: The derivative $\sigma_{j,i}'\equiv(\partial\sigma_j/\partial\upsilon_i)$, $i=1,\ldots,6$, of light switching event times σ_j, $j=1,2,\ldots$, with respect to the control parameters υ_i satisfies

$$\sigma_{j,i}'=\begin{cases}\dfrac{1}{\alpha_n(\sigma_j)}\cdot\left[\mathbf{1}[i=n+4]-x_{n,i}'\left(\sigma_j^-\right)\right] & \text{if } \zeta_n^b \text{ occurs at } \sigma_j\\ \dfrac{1}{\alpha_n(\sigma_j)-h_n(\sigma_j)}\cdot\left[\mathbf{1}[i=n+4]-x_{n,i}'\left(\sigma_j^-\right)\right] & \text{if } \zeta_n^a \text{ occurs at } \sigma_j\\ \mathbf{1}[i=2n-1]+\sigma_{j-1,i}', & \text{if } \lambda_n \text{ occurs at } \sigma_j\\ \mathbf{1}[i=2n]+\sigma_{j-1,i}', & \text{if } \mu_n \text{ occurs at } \sigma_j\\ \sigma_{j-1,i}', & \text{otherwise}\end{cases} \tag{19}$$

where $n=1,2$ and $\mathbf{1}[\cdot]$ is the usual indicator function.

Proof: We begin by considering the occurrence of a $G2R_n$ light switching event. Recall that this may be induced by one of the four endogenous events $\{\zeta_n^b,\zeta_n^a,\lambda_n,\mu_n\}$. Each of these cases will be separately analyzed in the following.

1) Event ζ_1^b Occurs at Time σ_j: This is an endogenous event that occurs when $x_1=s_1$ from below and results in a $G2R_2$ (hence, $R2G_1$) event as long as $z_2(\sigma_j)>\theta_{2,\min}$ and $x_2(\sigma_j)<s_2$ (see R1). Thus, in this case, the switching function in (15) is $g_j=x_1-s_1=0$, and we have $(\partial g_j/\partial x_1)=1$ and $(\partial g_j/\partial \upsilon_5)=-1$ [see (1)] with all the remaining partial derivatives equal to zero. Since $x_1(\sigma_j^-)<s_1$ and $x_1(\sigma_j^+)=s_1$, road 1 is necessarily in an NEP when this event takes place. Furthermore, the fact that road 1 is undergoing a RED phase at time σ_j^- but will be undergoing a GREEN phase at σ_j^+ means that $f_{1,j-1}^x(\sigma_j^-)=\alpha_1(\sigma_j)$ and $f_{1,j}^x(\sigma_j^+)=\alpha_1(\sigma_j)-h_1(\sigma_j)$ in (7). As a result, it is simple to verify that (15) reduces to

$$\sigma_{j,i}'=\begin{cases}\dfrac{1}{\alpha_1(\sigma_j)}\left[1-x_{1,i}'\left(\sigma_j^-\right)\right], & \text{if } i=5\\ \dfrac{-1}{\alpha_1(\sigma_j)}x_{1,i}'\left(\sigma_j^-\right), & \text{otherwise.}\end{cases} \tag{20}$$

2) Event ζ_2^b Occurs at Time σ_j: This is an endogenous event with $g_j=x_2-s_2=0$ from below, resulting in a $G2R_1$ event. The same reasoning as above applies to verify that (15) becomes

$$\sigma_{j,i}'=\begin{cases}\dfrac{1}{\alpha_2(\sigma_j)}\left[1-x_{2,i}'\left(\sigma_j^-\right)\right], & \text{if } i=6\\ \dfrac{-1}{\alpha_2(\sigma_j)}x_{2,i}'\left(\sigma_j^-\right), & \text{otherwise.}\end{cases} \tag{21}$$

3) Event ζ_1^a Occurs at Time σ_j: This is an endogenous event that occurs when $x_1=s_1$ from above and results in a $G2R_1$ event as long as $z_1(\sigma_j)>\theta_{1,\min}$ and $x_2(\sigma_j)\geq s_2$ (see R2). Thus, the switching function in (15) is $g_j=x_1-s_1=0$. In order for this event to take place at time σ_j, we must have $x_1(\sigma_j^-)>s_1$ and $x_1(\sigma_j^+)=s_1$, which means that road 1 must be in an NEP. Furthermore, since $x_2(\sigma_j)\geq s_2$, this implies that road 2 must also be in an NEP at σ_j. Since road 1 is undergoing a GREEN phase at time σ_j^- but will be undergoing a RED cycle at σ_j^+, we have $f_{1,j-1}^x(\sigma_j^-)=\alpha_1(\sigma_j)-h_1(\sigma_j)$

and $f^x_{1,j}(\sigma_j^+) = \alpha_1(\sigma_j)$ in (7). As a result, (15) can be seen to become

$$\sigma'_{j,i} = \begin{cases} \dfrac{1}{\alpha_1(\sigma_j) - h_1(\sigma_j)}\big[1 - x'_{1,i}(\sigma_j^-)\big], & \text{if } i = 5 \\ \dfrac{-1}{\alpha_1(\sigma_j) - h_1(\sigma_j)} x'_{1,i}(\sigma_j^-), & \text{otherwise.} \end{cases} \tag{22}$$

4) Event ζ_2^a Occurs at Time σ_j: This is an endogenous event with $g_j = x_2 - s_2 = 0$ from above, resulting in a $G2R_2$ event. The same reasoning as above applies to verify that (15) reduces to

$$\sigma'_{j,i} = \begin{cases} \dfrac{1}{\alpha_2(\sigma_j) - h_2(\sigma_j)}\big[1 - x'_{2,i}(\sigma_j^-)\big], & \text{if } i = 6 \\ \dfrac{-1}{\alpha_2(\sigma_j) - h_2(\sigma_j)} x'_{2,i}(\sigma_j^-), & \text{otherwise.} \end{cases} \tag{23}$$

5) Event λ_1 Occurs at Time σ_j: This is an endogenous event that occurs when $z_1 = \theta_{1,\min}$ and results in a $G2R_1$ event as long as $x_1(\sigma_j) < s_1$ and $x_2(\sigma_j) \geq s_2$ (see R3). Thus, the switching function in (15) is $g_j = z_1 - \theta_{1,\min} = 0$. Let $\tau_p < \sigma_j$ be the occurrence time of the last $R2G_1$ event before λ_1 takes place at time σ_j. It follows from (18) that $(d/dt)z'_{1,i}(t) = 0$, $i = 1, \ldots, 6$, for $t \in [\tau_p, \sigma_j)$, and therefore $z'_{1,i}(\sigma_j^-) = z'_{1,i}(\tau_p^+)$. Furthermore, the fact that road 1 is undergoing a RED phase at time τ_p^- but will be undergoing a GREEN phase at τ_p^+ means that $f^z_{1,p-1}(\tau_p^-) = 0$ and $f^z_{1,p}(\tau_p^+) = 1$ in (8).

Let $\tau_r < \tau_p$ also be the occurrence time of the last $G2R_1$ event before τ_p so that $z'_{1,i}(\tau_p^-) = z'_{1,i}(\tau_r^+)$ by a similar argument as above. Since $z_1(t)$ is reset to zero whenever a $G2R_1$ event takes place, we have $z'_{1,i}(\tau_r^+) = 0$. As a result, (14) can be easily seen to yield $z'_{1,i}(\tau_p^+) = -\tau'_{p,i}$, $i = 1, \ldots, 6$. Using a similar reasoning to the one applied for determining the change in state dynamics due to an $R2G_1$ event at τ_p, it is simple to verify that $f^z_{1,j-1}(\sigma_j^-) = 1$ and $f^z_{1,j}(\sigma_j^+) = 0$. By substituting these expressions into (15) and recalling that $\tau_p = \sigma_{j-1}$, we obtain

$$\sigma'_{j,i} = \begin{cases} 1 + \sigma'_{j-1,1}, & \text{if } i = 1 \\ \sigma'_{j-1,1}, & \text{otherwise.} \end{cases} \tag{24}$$

6) Event λ_2 Occurs at Time σ_j: This is an endogenous event with $g_j = z_2 - \theta_{2,\min} = 0$, resulting in a $G2R_2$ event. Let τ_r be the time of occurrence of the last $G2R_1$ event before λ_2 takes place at time σ_j. The same reasoning as above applies to verify that $z'_{2,i}(\sigma_j^-) = z'_{2,i}(\tau_r^+)$, $i = 1, \ldots, 6$. Furthermore, since light switches are coupled, road 2 is undergoing a RED phase at time τ_r^- but will be undergoing a GREEN phase at τ_r^+ so that $f^z_{2,r-1}(\tau_r^-) = 0$ and $f^z_{2,r}(\tau_r^+) = 1$. As a result, (14) yields $z'_{2,i}(\tau_r^+) = -\tau'_{r,i}$. By substituting these expressions into (15) and recalling that $\tau_p = \sigma_{j-1}$, we obtain

$$\sigma'_{j,i} = \begin{cases} 1 + \sigma'_{j-1,1}, & \text{if } i = 3 \\ \sigma'_{j-1,1}, & \text{otherwise.} \end{cases} \tag{25}$$

7) Event μ_1 Occurs at Time σ_j: This is an endogenous event that occurs when $z_1 = \theta_{1,\max}$ and always results in a $G2R_1$ event (see R3). Thus, the switching function in (15) is $g_j = z_1 - \theta_{1,\max} = 0$. The same reasoning as in Case 5 applies to verify that (15) reduces to

$$\sigma'_{j,i} = \begin{cases} 1 + \sigma'_{j-1,1}, & \text{if } i = 2 \\ \sigma'_{j-1,1}, & \text{otherwise.} \end{cases} \tag{26}$$

8) Event μ_2 Occurs at Time σ_j: This is an endogenous event with $g_j = z_2 - \theta_{2,\max} = 0$, resulting in a $G2R_2$ event. The same reasoning as in Case 6 applies to verify that (15) reduces to

$$\sigma'_{j,i} = \begin{cases} 1 + \sigma'_{j-1,1}, & \text{if } i = 4 \\ \sigma'_{j-1,1}, & \text{otherwise.} \end{cases} \tag{27}$$

■

We will use Proposition 1 in the following, where we consider each of the event types ($G2R_n$, $R2G_n$, E_n, and S_n).

1) *Event $G2R_n$:* The following two cases must be considered:
   a) *$G2R_n$ Occurs at τ_k While Road n Is Undergoing an NEP:* In this case, the fact that $x_n(\tau_k^-) > 0$ implies from (7) that $f_{n,k-1}(\tau_k^-) = \alpha_n(\tau_k) - h_n(\tau_k)$. In addition, since road n is undergoing a RED phase at time τ_k^+, we must have that $f^x_{n,k}(\tau_k^+) = \alpha_n(\tau_k)$. It follows from (14) that:
   $$x'_{n,i}(\tau_k^+) = x'_{n,i}(\tau_k^-) - h_n(\tau_k)\tau'_{k,i}$$
   for $n = 1, 2$ and $i = 1, \ldots, 6$.
   b) *$G2R_n$ Occurs at τ_k While Road n Is Undergoing an EP:* In this case, $x_n(\tau_k^-) = 0$, so that from (7), we have $f_{n,k-1}(\tau_k^-) = 0$, and it is simple to verify that
   $$x'_{n,i}(\tau_k^+) = x'_{n,i}(\tau_k^-) - \alpha_n(\tau_k)\tau'_{k,i}$$
   for $n = 1, 2$ and $i = 1, \ldots, 6$. Finally, if the kth event corresponds to the jth occurrence of a light switching event, we have that $\tau'_{k,i} = \sigma'_{j,i}$ for some $j = 1, 2, \ldots$. As a result, combining the two cases above, we get, for $n = 1, 2$ and $i = 1, \ldots, 6$
   $$x'_{n,i}(\tau_k^+) = x'_{n,i}(\tau_k^-) - \begin{cases} h_n(\tau_k)\sigma'_{j,i}, & \text{if } x_n(\tau_k) > 0 \\ \alpha_n(\tau_k)\sigma'_{j,i}, & \text{if } x_n(\tau_k) = 0 \end{cases} \tag{28}$$
   where $\sigma'_{j,i}$ is given by (19) in Proposition 1 with $\sigma_j = \tau_k$.

2) *Event $R2G_n$:* Once again, the following two cases must be considered:
   a) *$R2G_n$ Occurs at τ_k While Road n Is Undergoing an NEP:* In this case, the fact that road n is undergoing a RED phase within an NEP at time τ_k^- means that $f^x_{n,k-1}(\tau_k^-) = \alpha_n(\tau_k)$, and since it will be undergoing a GREEN phase at time τ_k^+, we must have that $f^x_{n,k}(\tau_k^+) = \alpha_n(\tau_k) - h_n(\tau_k)$. It follows from (14) that:
   $$x'_{n,i}(\tau_k^+) = x'_{n,i}(\tau_k^-) + h_n(\tau_k)\tau'_{k,i}$$
   for $n = 1, 2$ and $i = 1, \ldots, 6$.

b) *$R2G_n$ Occurs at τ_k While Road n Is Undergoing an EP:* In this case, the fact that road n is empty while undergoing a RED phase at time τ_k^- implies that $f^x_{n,k-1}(\tau_k^-) = \alpha_n(\tau_k)$ with $0 < \alpha_n(\tau_k) \leq h_n(\tau_k)$, while $f^x_{n,k}(\tau_k^+) = 0$ in (7), and it is simple to verify that

$$x'_{n,i}(\tau_k^+) = x'_{n,i}(\tau_k^-) + \alpha_n(\tau_k)\tau'_{k,i}$$

for $n = 1, 2$ and $i = 1, \ldots, 6$. Combining these two cases, we get, for $n = 1, 2$ and $i = 1, \ldots, 6$

$$x'_{n,i}(\tau_k^+) = x'_{n,i}(\tau_k^-) + \begin{cases} \alpha_n(\tau_k)\sigma'_{j,i}, & \text{if } x_n(\tau_k) = 0 \text{ and} \\ & 0 < \alpha_n(\tau_k) \leq h_n(\tau_k) \\ h_n(\tau_k)\sigma'_{j,i}, & \text{otherwise} \end{cases} \tag{29}$$

where again $\sigma'_{j,i}$ is given by (19) in Proposition 1 with $\sigma_j = \tau_k$.

3) *Event E_n:* This event corresponds to the end of an NEP on road n and is induced by χ_n, i.e., an endogenous event such that $x_n = 0$ from above. Thus, the switching function in (15) is $g_k = x_n = 0$. The fact that road n is in an NEP at time τ_k^- implies that $f^x_{n,k-1}(\tau_k^-) = \alpha_n(\tau_k) - h_n(\tau_k)$, and it follows from (15) that $\tau'_{k,i} = -(x'_{n,i}(\tau_k^-)/\alpha_n(\tau_k) - h_n(\tau_k))$. Furthermore, since road n is in an EP at time τ_k^+, we have that $f^x_{n,k}(\tau_k^+) = 0$ and (14) reduces to $x'_{n,i}(\tau_k^+) = x'_{n,i}(\tau_k^-) - x'_{n,i}(\tau_k^-)$ and we get

$$x'_{n,i}(\tau_k^+) = 0, \quad n = 1, 2 \quad \text{and} \quad i = 1, \ldots, 6. \tag{30}$$

4) *Event S_n:* This event corresponds to the start of an NEP on road n and can be induced either by a $G2R_n$ event, or γ_n^1 or γ_n^2. These three cases will be analyzed in the following.

a) *S_n Is Induced by a $G2R_n$ Event:* Suppose this is the start of the mth NEP on road n. This means that, during the preceding EP, which corresponds to the time interval $[\eta_{n,m-1}, \xi_{n,m})$, we have $x_n(t) = 0$ for $t \in [\eta_{n,m-1}, \xi_{n,m})$ and, consequently, $x'_{n,i}(t) = 0$ for $t \in [\eta_{n,m-1}, \xi_{n,m})$ and $i = 1, \ldots, 6$. Therefore, $x'_{n,i}(\eta^+_{n,m-1}) = x'_{n,i}(\xi^-_{n,m}) = 0$, and since τ_k corresponds to the time when the NEP starts on road n (i.e., $\tau_k = \xi_{n,m}$), it follows that $x'_{n,i}(\tau_k^-) = x'_{n,i}(\xi^-_{n,m}) = 0$. As a result, (28) can be easily seen to yield, for $n = 1, 2$ and $i = 1, \ldots, 6$

$$x'_{n,i}(\tau_k^+) = -\alpha_n(\tau_k)\tau'_{k,i}. \tag{31}$$

The value of $\tau'_{k,i}$ in (31) depends on the type of event that induced $G2R_n$. If the kth event corresponds to the jth light switching event, then $\tau'_{k,i} = \sigma'_{j,i}$, whose expression is given by (19). Note, however, that event S_n cannot be induced by ζ_n^a because the occurrence of event ζ_n^a is conditioned upon road n being in an NEP, and such a case is not possible here. As a result, the second case in (19) must be excluded.

b) *S_n Is Induced by a γ_n^2 Event:* Recall that γ_n^2 corresponds to a switch from $\alpha_n(t) = 0$ to $\alpha_n(t) > 0$ while road n is undergoing a RED phase, i.e., $z_n(t) = 0$. Since this is an exogenous event, $\tau'_{k,i} = 0$, $i = 1, \ldots, 6$, and (14) reduces to $x'_{n,i}(\tau_k^+) = x'_{n,i}(\tau_k^-)$. We know that the NEP starts on road n at time τ_k, so that $\tau_k = \xi_{n,m}$, and we have shown that $x'_{n,i}(\xi^-_{n,m}) = x'_{n,i}(\eta^+_{n,m-1}) = 0$. It thus follows that $x'_{n,i}(\tau_k^-) = x'_{n,i}(\xi^-_{n,m}) = 0$, so that $x'_{n,i}(\tau_k^+) = 0$, for $n = 1, 2$ and $i = 1, \ldots, 6$.

c) *S_n Is Induced by a γ_n^1 Event:* Event γ_n^1 corresponds to a switch from $\alpha_n(t) - h_n(t) \leq 0$ to $\alpha_n(t) - h_n(t) > 0$ while road n is undergoing a GREEN phase, i.e., $z_n(t) > 0$. Since this is an exogenous event, $\tau'_{k,i} = 0$, $i = 1, \ldots, 6$, and the subsequent analysis is similar to that of the previous case. As a result, $x'_{n,i}(\tau_k^+) = 0$, for $n = 1, 2$ and $i = 1, \ldots, 6$.

This completes the derivation of all the state and event time derivatives required to apply IPA to our TLC problem; the way in which the above derivatives are used to ultimately estimate $dJ/d\upsilon_i$, $i = 1, \ldots, 6$, will be detailed next.

B. Cost Derivatives

Returning to (10), recall that the IPA estimator consists of the gradient formed by the sample performance derivatives $dL/d\upsilon_i$. The following theorem provides the complete IPA estimator.

Theorem 1: The IPA estimator, i.e., the gradient of $L(\upsilon)$ consisting of $dL(\upsilon)/d\upsilon_i$, $i = 1, \ldots, 6$ is given by

$$\frac{dL(\upsilon)}{d\upsilon_i} = \frac{1}{T}\sum_{n=1}^{2}\sum_{m=1}^{M_n} \omega_n \frac{dL_{n,m}(\upsilon)}{d\upsilon_i}$$

where

$$\begin{aligned} L_{n,m}(\upsilon) &= \int_{\xi_{n.m}}^{\eta_{n,m}} x_n(\upsilon, t)dt \\ \frac{dL_{n,m}(\upsilon)}{d\upsilon_i} &= x'_{n,i}((\xi_{n.m})^+) \cdot \left(t^1_{n,m} - \xi_{n.m}\right) \\ &\quad + x'_{n,i}\left(\left(t^{J_{n,m}}_{n,m}\right)^+\right) \cdot \left(\eta_{n,m} - t^{J_{n,m}}_{n,m}\right) \\ &\quad + \sum_{j=2}^{J_{n,m}} x'_{n,i}\left(\left(t^j_{n,m}\right)^+\right) \cdot \left(t^j_{n,m} - t^{j-1}_{n,m}\right). \end{aligned} \tag{32}$$

Proof: From (10), we obtain

$$\frac{dL(\upsilon)}{d\upsilon_i} = \frac{1}{T}\sum_{n=1}^{2}\sum_{m=1}^{M_n}\int_{\xi_{n.m}}^{\eta_{n,m}} \omega_n x'_{n,i}(t)dt + \frac{1}{T}\sum_{n=1}^{2}\sum_{m=1}^{M_n} \times \left[\omega_n x_n(\eta_{n,m}) \cdot \frac{\partial \eta_{n,m}}{\partial \upsilon_i} - \omega_n x_n(\xi_{n.m}) \cdot \frac{\partial \xi_{n.m}}{\partial \upsilon_i}\right].$$

Since, by the definition of an NEP, road n is empty both at the start and end of an NEP, we have $x_n(\xi_{n,m}) = x_n(\eta_{n,m}) = 0$. Furthermore, we have shown in (18) that $x'_{n,i}(t)$ is piecewise constant throughout an NEP and its value changes only

Algorithm 1 IPA Algorithm for Quasi-Dynamic TLC

Whenever an event occurs at time τ_k**,** $k = 1, 2, \ldots$
if EVENT ζ_1^b [x_1 increases to s_1 from below]
  Update event time derivatives using (20)
else if EVENT ζ_1^a [x_1 decreases to s_1 from above]
  Update event time derivatives using (22)
else if EVENT λ_1 [green time z_1 reaches $\theta_{1,\min}$]
  Update event time derivatives using (24)
else if EVENT μ_1 [green time z_1 reaches $\theta_{1\max}$]
  Update event time derivatives using (26)
endif
if event is $G2R_1$ or $R2G_1$ [green switches to red or vice versa]
  Update state derivatives using (28) and (29)
else if EVENT χ_1 [queue 1 becomes empty]
  Update state derivatives of road 1 using (30)
endif
Update cost derivatives using (32) for $i = 1, \ldots, 6$.
End

at instants when events take place. This implies that we can decompose each NEP into time intervals of the form $[\xi_{n.m}, t^1_{n,m})$, $[t^1_{n,m}, t^2_{n,m}), \ldots, [t^{J_{n,m}}_{n,m}, \eta_{n,m})$. Using the definition of $L_{n,m}(\upsilon)$, (32) immediately follows. ■

C. Implementation Issues

It is clear from (32) that evaluating the IPA estimator requires knowledge of: 1) the event times $\xi_{n.m}$, $\eta_{n,m}$, and $t^j_{n,m}$ and 2) the value of the state derivatives $x'_{n,i}(t)$ at event times $t = \xi_{n.m}$, $t = t^{J_{n,m}}_{n,m}$, and $t = t^j_{n,m}$. The quantities in 1) are easily observed using timers whose start and end times are observable events. The state derivatives in 2) are obtained from the expressions derived in (28) and (31) for $G2R_n$ light switching events, (29) for $R2G_n$ light switching events, and $x'_{n,i}(\tau_k^+) = 0$ for all other events occurring at $t = \tau_k$. Ultimately, these expressions depend on the values of the arrival and departure rates $\alpha_n(t)$ and $h_n(t)$ at light switching event times *only*, which may be estimated through simple rate estimators.

As a result, it is straightforward to implement an algorithm for updating the value of $dL(\upsilon)/d\upsilon_i$ after each observed event, as outlined in Algorithm 1. For conciseness, only the events occurring on road 1 are shown (note that, since events γ_1^1 and γ_1^2 have a null effect on the state derivatives, it is not necessary to check for their occurrence).

We also point out that our IPA estimator is linear in the number of events in the SFM, not in its states. This is a crucial observation because it implies that our approach scales with the number of traffic lights in a network of interconnected intersections. Another crucial observation is that the IPA estimator depends only on events that are observable in the actual intersection operating as a DES; for example, event χ_n is simply the condition [$x_n = 0$ from above], i.e., an event representing the fact that a road queue becomes empty. In other words, even though the IPA estimator is derived from our SFM (7), (8), its actual implementation is entirely driven by actually observed events in the real intersection.

Extending the proposed controller to incorporate bidirectional and left/right turn traffic is straightforward, requiring the addition of variables that capture associated traffic flows and of parameters for the green/red times and backlog thresholds. The extension to multiple intersections is also a direct one as shown in [24] and includes phenomena arising when upstream traffic flow is blocked by a congested neighboring intersection; in fact, IPA equations explicitly capture such effects. However, our simple model (7), (8) will have to be enhanced to incorporate acceleration and deceleration delays, as well as delays in vehicles reaching a downstream traffic light dependent on the length between adjacent intersections and the state of the associated queues.

We also point out that our traffic light controller does not assume a fixed cycle consisting of red and green phases, i.e., setting $T = R + G$, where T is fixed. This a special case of our model, which can be easily incorporated in our analysis as shown in [22] by simply constraining the red and green phases to add up to T and treating T, if desired, as a controllable parameter. This allows us to study the coordination of multiple traffic lights in series and achieve the so-called green waves whereby vehicles maximize their chance of encountering a green light over several intersections in a row.

As already mentioned, the purpose of this paper is to demonstrate the advantages of quasi-dynamic TLC using IPA techniques before expanding this effort to networks of urban roadways and multidirectional traffic flows. It is for this reason that all the simulation results reported in the next section were obtained based on a simple simulator we developed, as opposed to commercial traffic network simulators (e.g., VISSIM). As we extend this work to multiple intersections and include the additional features discussed above, we will be incorporating our controllers to such commercial simulators.

We end with a conceptual comparison of our methodology with some well-known approaches (e.g., Webster's method [9], SIGSET, and SIGCAP [28]). Since these approaches are fixed-time strategies, they must rely on historical data to determine and preset signal timings, and therefore signal cycles cannot be automatically adjusted to handle fluctuating vehicle flows [19]. Our methodology, on the other hand, allows for the design of fully actuated signals, whose settings can be changed online to account for random traffic variations. In fact, our IPA algorithm can be implemented online and is thus capable of processing real-time traffic data, while the algorithms that result from the aforementioned strategies must be solved offline using historical data. Finally, we stress that, although we have not implemented the Webster, SIGSET, and SIGCAP algorithms, a comparison of the simulation results obtained through our methodology and those obtained using fixed-time strategies is given in Table I.

IV. Simulation Results

In what follows, we detail how an IPA-driven gradient-based optimization approach can simultaneously control the green and red light times and the queue content thresholds for a single traffic light intersection, which is modeled as a DES. Two sets of simulations were performed: one in which

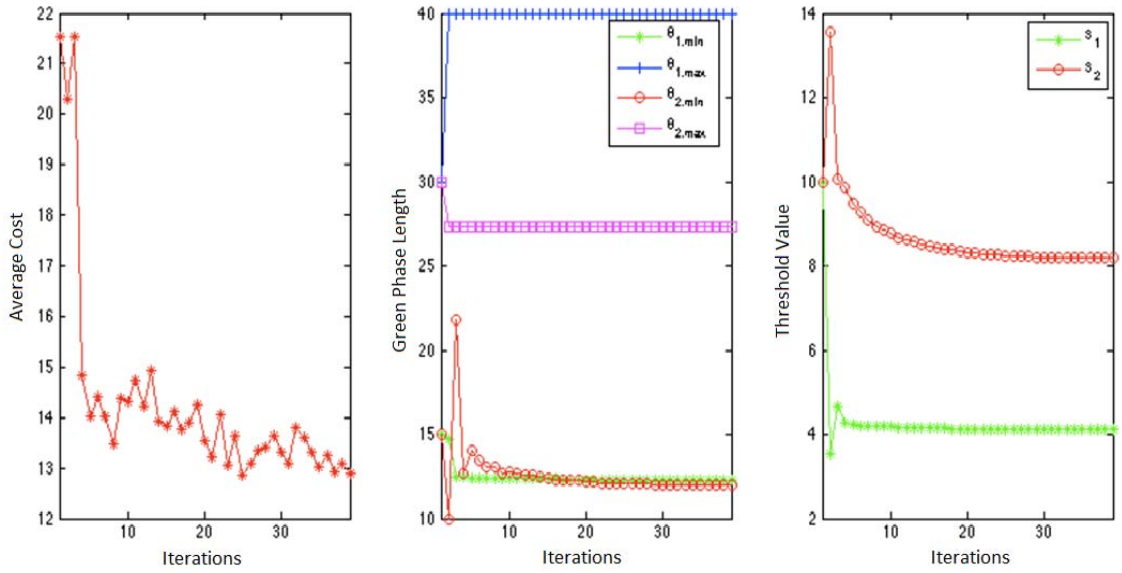

Fig. 6. Sample cost and parameter trajectories for $1/\bar{\alpha} = [1.7, 3]$.

TABLE I
OPTIMIZATION RESULTS FOR DIFFERENT TRAFFIC INTENSITIES

$1/\bar{\alpha}$	θ^*_{IPA}	$\mathbf{s}^*_{IPA}$	J^*_{IPA}	$R(\%)$
$[1.7, 3]$	$[12.3, 39.9, 12, 27.3]$	$[4.1, 8.2]$	12.9	46
$[1.8, 3]$	$[12.8, 30.8, 10, 29.9]$	$[3.6, 4.1]$	10	47
$[1.9, 3]$	$[14.4, 30, 11.2, 29.9]$	$[5.4, 6.6]$	8.9	47
$[2, 3]$	$[13.3, 29.9, 10, 30]$	$[3.8, 4.4]$	7.7	47
$[2.2, 2.7]$	$[14.5, 30, 12.8, 30]$	$[6.3, 6.9]$	8.5	57
$[2, 6]$	$[15, 31.5, 12.1, 29.9]$	$[5.7, 9.9]$	5.6	48

the same initial phase length/threshold setting was used for different traffic intensities and another in which different starting points were used for the given values of traffic intensity.

In all our simulations, we assume that the vehicle arrival process is Poisson with rate $\bar{\alpha}_n, n = 1, 2$, and approximate the departure rate by a constant value $h_n(t) = H$ when road n is nonempty (this ignores acceleration effects and the interdependence of queued vehicles). We nevertheless remind the reader that our methodology applies independently of the distribution chosen to represent the arrival and departure processes, which we need only assume to be piecewise continuous w.p. 1. We estimate the values of the arrival rate at event times as $\alpha_n(\tau_k) = N_a/t_w$, where N_a corresponds to the number of vehicle arrivals during a time window of size t_w just before τ_k. We also note that we consider $h_n(t) = H$ throughout the numerical simulations for simplicity; if the value of $h_n(t)$ were not taken to be constant, we would simply need to estimate it at event times only (exactly as we do for $\bar{\alpha}_n$). Simulations of the intersection modeled as a pure DES are thus run to generate sample path data to which the IPA estimator is applied. In all the results reported here, we set $H = 1$, $w_n = 1$, and $n = 1, 2$, and measure the sample path length in between updates of the controllable parameter vector v in terms of the number of observed light switches, which we choose to be $N = 5000$.

In our first set of simulations, the initial configuration was chosen to be $\theta_0 = [15, 30, 15, 30]$ and $s_0 = [10, 10]$. Table I presents the optimization results associated with different traffic intensities (denoted by $1/\bar{\alpha}$), where θ^*_{IPA} and $\mathbf{s}^*_{\text{IPA}}$ denote the optimal phase lengths and threshold values, respectively, and J^*_{IPA} is the cost associated with the optimal configuration. We also include here a comparison of the results generated by our methodology with those obtained when static control [22] is applied to determine the optimal phase lengths. This is captured by $R(\%)$ in Table I, the fractional cost reduction achieved by our method with respect to the static approach. The static controller defined in [22] adjusts the green light times subject to some lower and upper bounds and determines $\theta^*_{\text{static}} = [\theta^*_1, \theta^*_2]$, where θ^*_1 (θ^*_2, respectively) is the green phase length that should be allotted to road 1 (road 2, respectively) so as to minimize the average queue content on both roads. The advantage of quasi-dynamically controlling the light cycle lengths and threshold values over a static IPA approach to the TLC problem was established in [17]. However, in [17], we made use of a sequential optimization procedure, where first the optimal phase lengths were determined considering fixed threshold values, and then the queue content thresholds were optimized. The magnitude of the cost reduction obtained using this approach varied in the range 38%–51%. We have found that performing a *simultaneous* optimization of both phase lengths and threshold values provides a cost reduction that is in most cases at least as high as the aforementioned sequential approach. Indeed, for $1/\bar{\alpha} = [1.7, 3]$, sequential optimization yielded a 38% cost reduction, while our simultaneous optimization method allowed for a reduction of 46%, and for $1/\bar{\alpha} = [2, 3]$, both approaches resulted in a comparable overall cost, which was 47% lower than the one obtained under static control for the simultaneous optimization and 51% lower in the case of sequential optimization. Moreover, our methodology consistently yields results in which the traffic buildup at the intersection is approximately half the size of the one under static control.

The convergence behavior of the cost and the controllable phase lengths and threshold parameters are shown in Figs. 6 and 7. The left plot of Figs. 6 and 7 shows the average cost, which in this paper corresponds to the weighted mean of the queue length of both roads, while the middle and

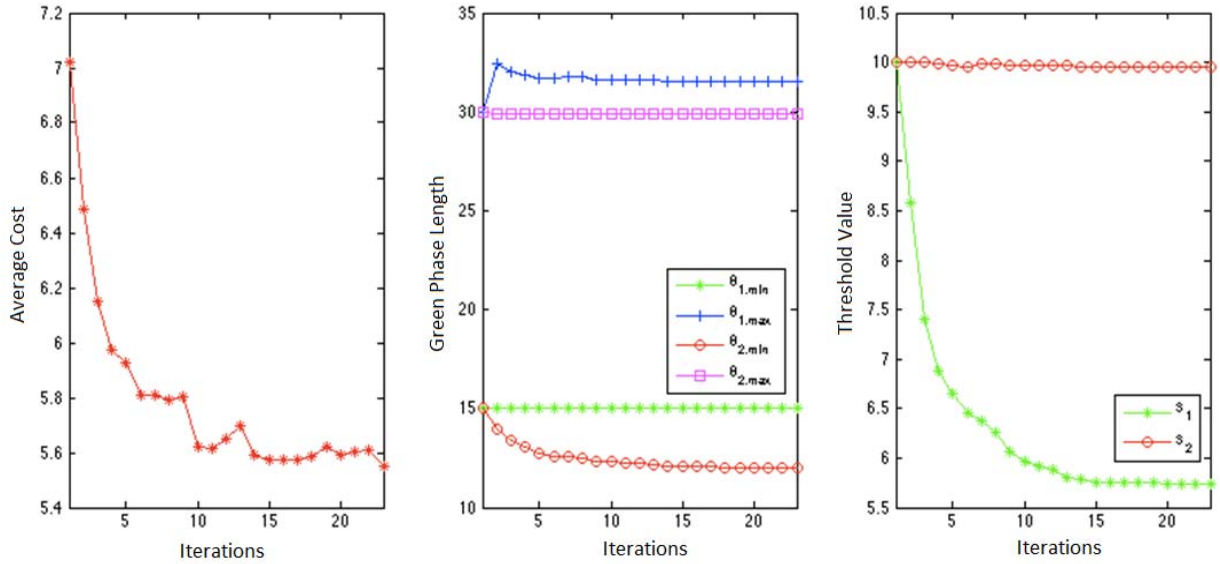

Fig. 7. Sample cost and parameter trajectories for $1/\bar{\alpha} = [2, 6]$.

TABLE II

CONVERGENCE RESULTS FOR DIFFERENT INITIAL CONFIGURATIONS

	Initial configuration	Optimal configuration		
$1/\overline{\alpha}$	v_0	v^*_{opt}	J^*_{opt}	*Fractional Cost Reduction* (%)
$[1.7, 3]$	$[15, 30, 15, 30, 10, 10]$	$[12.3, 39.9, 12, 27.3, 4.1, 8.2]$	12.9	46
	$[10, 20, 10, 20, 5, 5]$	$[10, 39.9, 10.9, 19.3, 2.3, 6.1]$	12.6	47
	$[10, 20, 10, 30, 10, 5]$	$[10, 39.9, 11.2, 28.9, 5.7, 8.3]$	12.7	47
$[1.8, 3]$	$[15, 30, 15, 30, 10, 10]$	$[12.8, 30.8, 10, 29.9, 3.6, 4.1]$	10	47
	$[10, 20, 10, 20, 5, 5]$	$[10, 23, 10, 18.8, 4.6, 5.1]$	10.2	49
	$[10, 20, 10, 30, 10, 5]$	$[10.5, 33.4, 10.5, 27.9, 5.3, 7.0]$	10.5	45
$[1.9, 3]$	$[15, 30, 15, 30, 10, 10]$	$[14.4, 30, 11.2, 29.9, 5.4, 6.6]$	8.9	47
	$[10, 20, 10, 20, 5, 5]$	$[10, 21.9, 10, 19.5, 3.6, 4.7]$	8.6	49
	$[10, 20, 10, 30, 10, 5]$	$[11, 26.3, 10, 28.3, 4.6, 5.8]$	8.7	48

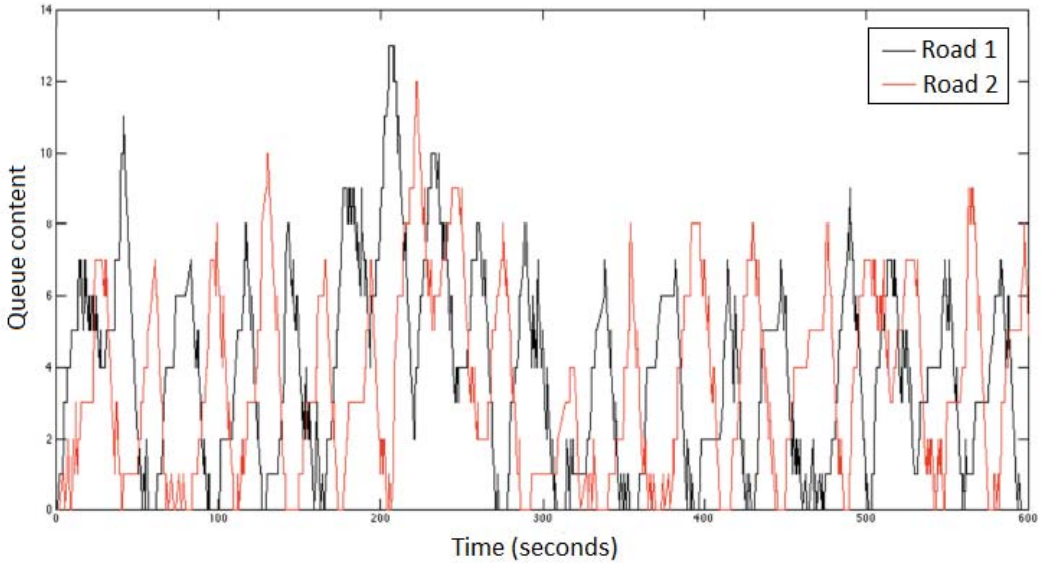

Fig. 8. Simulated traffic flow variation for $1/\bar{\alpha} = [2.2, 2.7]$.

right plots display the convergence behavior of the green phase lengths and threshold values, respectively. It is worthwhile to note that, in most of the analyzed scenarios, the value of the average cost converges much more slowly than the values of the controllable parameters, but we remind the reader that the purpose of our work is precisely to identify controllable parameters whereby an effective quasi-dynamic TLC may be imposed. As such, existing oscillations in the average cost value, albeit small once the green phase lengths and threshold values have converged, point to the robustness of our proposed approach. We also draw the reader's attention to the difference in the convergence time between the green phase length parameters and threshold parameters. It can be observed in Figs. 6 and 7 that the real challenge in convergence lies

with the threshold values, which represent the quasi-dynamic parameters introduced by our methodology, while the green phase lengths generally converge much faster to their optimal configuration.

In our second set of simulations, we analyze the convergence results in light of the existence of local minima, and three different traffic intensity settings are contemplated. Table II summarizes the results obtained when different initial configurations (θ_0 and $\mathbf{s}_0$ values) are used. It comes as no surprise that local minima exist throughout the 6-D cost surface of this system so that the optimal configuration to which the algorithm converges is dependent on the starting point. More interesting, however, is the fact that, for any given traffic intensity, we are able to consistently achieve a cost reduction of the order of 50% across different optimal configurations.

We also include an example of the simulated traffic flow variation in Fig. 8, which presents the queue content on both roads as a function of the simulation time. For ease of visualization, the entire sample path length in between updates of the controllable parameters is not shown in Fig. 8. Nevertheless, it is possible to note that the queue lengths on both roads become increasingly bounded as the simulation progresses. This indicates that, as the algorithm converges to optimal phase length and threshold settings, the number of vehicles on each road tends to oscillate within tighter bounds, whose values are directly related to the optimal threshold values determined for each road.

V. Conclusion

We have modeled a single traffic light intersection as an SFM and formulated the corresponding TLC problem within a quasi-dynamic control setting to which IPA techniques were applied in order to derive gradient estimates of a cost metric with respect to controllable phase lengths and queue content threshold values. By subsequently incorporating these estimators into a gradient-based optimization algorithm and simultaneously determining the optimal phase length/threshold configuration, we were able to reduce traffic buildup by approximately half (with respect to the traffic buildup resulting from a system operating under static control). Such results were consistently observed across a range of different traffic intensity settings and provide strong evidence of the advantages of applying an IPA-based quasi-dynamic control framework to the TLC problem. Our ongoing research is now focused on applying IPA to an intersection with more complicated traffic flows, e.g., allowing for left and right turns. The presence of more competing flows implies the need for also controlling the light phase sequence, which our methodology can handle by defining additional parameters (e.g., redefining the control vector θ by adding constraints that dictate the number of mutually exclusive flows). We are also aiming to incorporate acceleration/deceleration due to light switches into the model, as well as extending our methodology to a network of multiple intersections. Assuming that traffic lights can communicate with each other, it is also possible to endow a downstream light with the ability to predict an impending flow of vehicles and adjust its light cycle within the proposed quasi-dynamic framework, i.e., by adjusting its threshold parameters accordingly. Finally, it is worth acknowledging the emergence of a virtual traffic light setting [43], in which case IPA techniques are equally applicable to the switching control of a virtual rather than actual traffic light.

References

[1] B. Abdulhai, R. Pringle, and G. J. Karakoulas, "Reinforcement learning for *true* adaptive traffic signal control," *J. Transp. Eng.*, vol. 129, no. 3, pp. 278–285, 2003.

[2] I. Alvarez and A. Poznyak, "Game theory applied to urban traffic control problem," in *Proc. Int. Conf. Control, Autom. Syst.*, Oct. 2010, pp. 2164–2169.

[3] A. L. C. Bazzan, "Opportunities for multiagent systems and multiagent reinforcement learning in traffic control," *Auto. Agents Multi-Agent Syst.*, vol. 18, no. 3, pp. 342–375, Jun. 2009.

[4] C. G. Cassandras, "Event-driven control and optimization in hybrid systems," in *Event-Based Control and Signal Processing*. Boca Raton, FL, USA: CRC Press, 2015, To appear.

[5] C. G. Cassandras and S. Lafortune, *Introduction to Discrete Event Systems*. New York, NY, USA: Springer-Verlag, 2008.

[6] C. G. Cassandras, Y. Wardi, B. Melamed, G. Sun, and C. G. Panayiotou, "Perturbation analysis for online control and optimization of stochastic fluid models," *IEEE Trans. Autom. Control*, vol. 47, no. 8, pp. 1234–1248, Aug. 2002.

[7] C. G. Cassandras, Y. Wardi, C. G. Panayiotou, and C. Yao, "Perturbation analysis and optimization of stochastic hybrid systems," *Eur. J. Control*, vol. 16, no. 6, pp. 642–661, 2010.

[8] W. Choi, H. Yoon, K. Kim, I. Chung, and S. Lee, "A traffic light controlling FLC considering the traffic congestion," in *Proc. AFSS Int. Conf. Fuzzy Syst.*, 2002, pp. 69–75.

[9] U.S. Department of Transportation Federal Highway Administration. (2013). *Traffic Signal Timing Manual*. [Online]. Available: http://ops.fhwa.dot.gov/publications/fhwahop08024.htm

[10] C. Dong, "Area traffic signal timing optimization based on chaotic and genetic algorithm approach," *Comput. Eng. Appl.*, vol. 40, no. 29, pp. 32–34, 2004.

[11] C. Dong, "Chaos-particle swarm optimization algorithm and its application to urban traffic control," *Int. J. Comput. Sci. Netw. Secur.*, vol. 61, no. 1, pp. 97–101, 2006.

[12] C. Dong, Z. Liu, and Z. Qiu, "Urban traffic signal timing optimization based on multi-layer chaos neural networks involving feedback," in *Proc. 1st Int. Conf. Natural Comput.*, 2005, pp. 340–344.

[13] F. Dressler, H. Hartenstein, O. Altintas, and O. Tonguz, "Inter-vehicle communication: Quo vadis," *IEEE Commun. Mag.*, vol. 52, no. 6, pp. 170–177, Jun. 2014.

[14] Y. Dujardin, F. Boillot, D. Vanderpooten, and P. Vinant, "Multiobjective and multimodal adaptive traffic light control on single junctions," in *Proc. IEEE Int. Conf. Intell. Transp. Syst.*, Oct. 2011, pp. 1361–1368.

[15] N. V. Findle, S. Surender, and Ş. Catrava, "On-line decisions about permitted/protected left-hand turns in distributed traffic signal control," *Eng. Appl. Artif. Intell.*, vol. 10, no. 3, pp. 315–320, Jun. 1997.

[16] N. V. Findler and J. Stapp, "Distributed approach to optimized control of street traffic signals," *J. Transp. Eng.*, vol. 118, no. 1, pp. 99–110, Jan. 1992.

[17] J. L. Fleck and C. G. Cassandras, "Infinitesimal perturbation analysis for quasi-dynamic traffic light controllers," in *Proc. Int. Workshop Discrete Event Syst.*, 2014, pp. 235–240.

[18] M. C. Fu and W. C. Howell, "Application of perturbation analysis to traffic light signal timing," in *Proc. IEEE Conf. Decision Control*, Dec. 2003, pp. 4837–4840.

[19] N. J. Garber and L. A. Hoel, *Traffic and Highway Engineering*, 4th ed. Boston, MA, USA: Cengage Learning, 2009.

[20] N. H. Gartner, "OPAC: A demand responsive strategy for traffic signal control," *J. Transp. Res. Board*, vol. 1, no. 906, pp. 75–81, 1983.

[21] Y. Geng and C. G. Cassandras, "Multi-intersection traffic light control using infinitesimal perturbation analysis," in *Proc. Int. Workshop Discrete Event Syst.*, 2012, pp. 104–109.

[22] Y. Geng and C. G. Cassandras, "Traffic light control using infinitesimal perturbation analysis," in *Proc. IEEE Conf. Decision Control*, Dec. 2012, pp. 7001–7006.

[23] Y. Geng and C. G. Cassandras. (2013). "Quasi-dynamic traffic light control for a single intersection." [Online]. Available: http://arxiv.org/abs/1308.0864
[24] Y. Geng and C. G. Cassandras, "Multi-intersection traffic light control with blocking," *J. Discrete Event Dyn. Syst.*, vol. 25, nos. 1–2, pp. 7–30, Jun. 2015.
[25] L. Head, F. Ciarallo, and D. L. Kaduwela, "A perturbation analysis approach to traffic signal optimization," in *INFORMS Nat. Meeting*, 1996.
[26] J. J. Henry and J. L. Farges, "PRODYN," in *Proc. IFAC/IFIP/IFORS Symp.*, Paris, France, Sep. 1989, pp. 253–255.
[27] J. J. Henry, J. L. Farges, and J. L. Gallego, "Neuro-fuzzy techniques for traffic control," *Control Eng. Pract.*, vol. 6, no. 6, pp. 755–761, Jun. 1998.
[28] W. C. Howell and M. C. Fu. (2006). *Simulation Optimization of Traffic Light Signal Timings via Perturbation Analysis*. [Online]. Available: http://citeseerx.ist.psu.edu/viewdoc/summary?doi=10.1.1.362.3837
[29] P. B. Hunt, D. I. Robertson, R. D. Bretherton, and M. C. Royle, "The SCOOT on-line traffic signal optimization technique," in *Proc. Int. Conf. Road Traffic Signaling*, Mar./Apr. 1982, pp. 59–62.
[30] J. D. C. Little, M. D. Kelson, and N. H. Gartner, "MAXBAND: A program for setting signals on arteries and triangular networks," in *Proc. Transp. Res. Rec. 795, Traffic Flow Theory Characteristics*, 1981, pp. 40–46.
[31] Z. Liu, "A survey of intelligence methods in urban traffic signal control," *Int. J. Comput. Sci. Netw. Secur.*, vol. 7, no. 7, pp. 105–112, 2007.
[32] P. R. Lowrie, "The Sydney coordinated adaptive traffic system—Principles, methodology, algorithms," in *Proc. IEE Conf. Road Traffic Signaling*, 1982, pp. 67–70.
[33] C. G. Panayiotou, W. C. Howell, and M. C. Fu, "Online traffic light control through gradient estimation using stochastic fluid models," in *Proc. IFAC Triennial World Congr.*, Jul. 2005.
[34] C. P. Pappis and E. H. Mamdani, "A fuzzy logic controller for a traffic junction," *IEEE Trans. Syst., Man, Cybern.*, vol. 7, no. 10, pp. 707–717, Oct. 1977.
[35] I. Porche, M. Sampath, R. Sengupta, Y.-L. Chen, and S. Lafortune, "A decentralized scheme for real-time optimization of traffic signals," in *Proc. IEEE Int. Conf. Control Appl.*, Sep. 1996, pp. 582–589.
[36] L. A. Prashanth and S. Bhatnagar, "Reinforcement learning with function approximation for traffic signal control," *IEEE Trans. Intell. Transp. Syst.*, vol. 12, no. 2, pp. 412–421, Jun. 2011.
[37] D. I. Robertson, "TRANSYT method for area traffic control," *Traffic Eng. Control*, vol. 11, no. 6, pp. 276–281, 1969.
[38] B. De Schutter, "Optimal traffic light control for a single intersection," in *Proc. Amer. Control Conf.*, Jun. 1999, pp. 2195–2199.
[39] S. Sen and K. L. Head, "Controlled optimization of phases at an intersection," *Transp. Sci.*, vol. 31, no. 1, pp. 5–17, 1997.
[40] S. G. Shelby, D. M. Bullock, D. Gettman, R. S. Ghaman, Z. A. Sabra, and N. Soyke, "An overview and performance evaluation of ACS lite—A low cost adaptive signal control system," in *Proc. 87th Annu. Meeting Transp. Res. Board*, Jan. 2008.
[41] J. C. Spall and D. C. Chin, "Traffic-responsive signal timing for system-wide traffic control," *Transp. Res. C, Emerg. Technol.*, vol. 5, nos. 3–4, pp. 153–163, Aug./Oct. 1997.
[42] T. Tettamanti, T. Luspay, B. Kulcsar, T. Peni, and I. Varga, "Robust control for urban road traffic networks," *IEEE Trans. Intell. Transp. Syst.*, vol. 15, no. 1, pp. 385–398, Feb. 2014.
[43] O. Tonguz, W. Viriyasitavat, and J. Roldan, "Implementing virtual traffic lights with partial penetration: a game-theoretic approach," *IEEE Commun. Mag.*, vol. 52, no. 12, pp. 173–182, 2014.
[44] S. V. Ukkusuri, G. Ramadurai, and G. Patil, "A robust transportation signal control problem accounting for traffic dynamics," *Comput. Oper. Res.*, vol. 37, no. 5, pp. 869–879, May 2010.
[45] Y. Wardi, R. Adams, and B. Melamed, "A unified approach to infinitesimal perturbation analysis in stochastic flow models: The single-stage case," *IEEE Trans. Autom. Control*, vol. 55, no. 1, pp. 89–103, Jan. 2010.
[46] W. Wen, "A dynamic and automatic traffic light control expert system for solving the road congestion problem," *Expert Syst. Appl.*, vol. 34, no. 4, pp. 2370–2381, 2008.
[47] Y. Wen and T. Wu, "Reduced-order rolling horizon optimization of traffic control based on ant algorithm," *J. Zhejiang Univ. (Eng. Sci.)*, vol. 39, no. 6, pp. 835–839, 2005.
[48] W.-M. Wey, "Model formulation and solution algorithm of traffic signal control in an urban network," *Comput., Environ. Urban Syst.*, vol. 24, no. 4, pp. 355–378, Jul. 2000.
[49] M. Wiering, J. van Veenen, J. Vreeken, and A. Koopman, "Intelligent traffic light control," Inst. Inf. Comput. Sci., Utrecht Univ., Utrecht, The Netherlands, Tech. Rep. UU-CS-2004-029, 2004.
[50] C. Yao and C. G. Cassandras, "Perturbation analysis of stochastic hybrid systems and applications to resource contention games," *Frontiers Elect. Electron. Eng. China*, vol. 6, no. 3, pp. 453–467, Sep. 2011.
[51] Y. Yin, "Robust optimal traffic signal timing," *Transp. Res. B, Methodol.*, vol. 42, no. 10, pp. 911–924, Dec. 2008.
[52] X.-H. Yu and W. W. Recker, "Stochastic adaptive control model for traffic signal systems," *Transp. Res. C, Emerg. Technol.*, vol. 14, no. 4, pp. 263–282, Aug. 2006.
[53] X. Zhao and Y. Chen, "Traffic light control method for a single intersection based on hybrid systems," in *Proc. IEEE Int. Conf. Intell. Transp. Syst.*, Oct. 2003, pp. 1105–1109.

Julia L. Fleck received the B.Eng. degree in chemical engineering from the Federal University of Rio de Janeiro, Rio de Janeiro, Brazil, in 2006, and the M.S. degree in mechanical engineering from the Catholic University of Rio de Janeiro, Rio de Janeiro, in 2008. She is currently pursuing the Ph.D. degree with the Division of Systems Engineering, Boston University, Brookline, MA, USA.

She was a Researcher with Tecgraf/PUC-Rio, Rio de Janeiro, from 2008 to 2011, where she was involved in the development of artificial intelligence algorithms for enhanced oil recovery. Her current research interests include stochastic hybrid systems, optimal control, and stochastic optimization.

Christos G. Cassandras (F'96) received the B.S. degree from Yale University, New Haven, CT, USA, in 1977, the M.S.E.E. degree from Stanford University, Stanford, CA, USA, in 1978, and the M.S. and Ph.D. degrees from Harvard University, Cambridge, MA, USA, in 1979 and 1982, respectively.

He was with ITP Boston, Inc., Cambridge, from 1982 to 1984, where he was involved in the design of automated manufacturing systems. From 1984 to 1996, he was a Faculty Member with the Department of Electrical and Computer Engineering, University of Massachusetts Amherst, Amherst, MA, USA. He is currently a Distinguished Professor of Engineering with Boston University, Brookline, MA, USA, the Head of the Division of Systems Engineering, and a Professor of Electrical and Computer Engineering. He specializes in the areas of discrete event and hybrid systems, cooperative control, stochastic optimization, and computer simulation, with applications to computer and sensor networks, manufacturing systems, and transportation systems. He has authored over 350 refereed papers in these areas, and five books.

Dr. Cassandras is a member of Phi Beta Kappa and Tau Beta Pi. He is also a fellow of the International Federation of Automatic Control (IFAC). He was a recipient of several awards, including the 2011 IEEE Control Systems Technology Award, the 2006 Distinguished Member Award of the IEEE Control Systems Society, the 1999 Harold Chestnut Prize (IFAC Best Control Engineering Textbook), a 2011 prize and a 2014 prize for the IBM/IEEE Smarter Planet Challenge competition, the 2014 Engineering Distinguished Scholar Award at Boston University, several honorary professorships, a 1991 Lilly Fellowship, and a 2012 Kern Fellowship. He was the Editor-in-Chief of the IEEE TRANSACTIONS ON AUTOMATIC CONTROL from 1998 to 2009. He serves on several editorial boards and has been a Guest Editor for various journals. He was the President of the IEEE Control Systems Society in 2012.

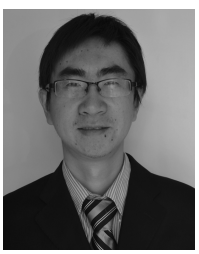

Yanfeng Geng (S'11) received the B.S. degree from the University of Science and Technology of China, Hefei, China, in 2005, and the Ph.D. degree from the Division of Systems Engineering, Boston University, Brookline, MA, USA, in 2013.

He is currently with Amazon in Boston, MA, USA. His current research interests include intelligent transportation system, optimal control, and stochastic optimization.